Available online at www.sciencedirect.com
SCIENCE DIRECT®
Journal of Solid State Chemistry 178 (2005) 1064–1070
JOURNAL OF SOLID STATE CHEMISTRY
www.elsevier.com/locate/jssc

Optical properties of $(Y_{1-x}Tm_x)_3GaO_6$ and subsolidus phase relation of Y_2O_3–Ga_2O_3–Tm_2O_3

F.S. Liu[a,b,*], B.J. Sun[b], J.K. Liang[b,c], Q.L. Liu[b,*], J. Luo[b], Y. Zhang[b], L.X. Wang[d], J.N. Yao[d], G.H. Rao[b]

[a]School of Material Science and Engineering, Southwest University of Science and Technology, Mianyang 621002, China
[b]Institute of Physics and Center for Condensed Matter Physics, Chinese Academy of Sciences, Beijing 100080, China
[c]International Centre for Materials Physics, Academia Sinica, Shenyang 110016, China
[d]Institute of Chemistry, Chinese Academy of Sciences, Beijing 100080, China

Received 8 October 2004; received in revised form 10 January 2005; accepted 11 January 2005

Abstract

A serial of samples in Y_2O_3–Ga_2O_3–Tm_2O_3 pseudo-ternary system are prepared by solid-state chemical reaction method. The range of solid solution in $(Y_{1-x}Tm_x)_3GaO_6$ is $0<x<0.384$. Powder X-ray diffraction shows that the compounds crystallize in Gd_3GaO_6 ($Cmc2_1$)-type structure. The solid solubilities of $Y_{3+x}Ga_{5-x}O_{12}$ ($x=0$–0.77) and $Tm_{3+x}Ga_{5-x}O_{12}$ ($x=0$–0.62) are 37.5–47.11 at% Y_2O_3, and 37.5–45.26 at% Tm_2O_3, respectively. PL spectra of Tm-doped Y_3GaO_6 show that there is a sharp blue emission at ~456 nm from the $^1D_2\rightarrow{}^3F_4$ transition at room temperatures with two lifetimes (~5 and ~15 μs) and a narrow saturation range of PL intensity for the Tm^{3+} content from $x=0.005$ to 0.03. The sharp emission and long lifetime of $(Y_{1-x}Tm_x)_3GaO_6$ indicate that Y_3GaO_6 is a potential phosphor and laser crystal host material.

PACS: 61.10.Nz; 61.66.Fn; 78.55.Hx

Keyword: Tm^{3+}-doped Y_3GaO_6; Y_2O_3–Ga_2O_3–Tm_2O_3 system; $(Y_{1-x}Tm_x)_3Ga_5O_{12}$ solid solution; Luminescence

1. Introduction

Rare-earth-doped materials are of special importance for optoelectronics and widely employed in fibre amplifiers, solid-state lasers and phosphors. The rare-earth ions are characterized by a partially filled $4f$ shell that is shielded by $5s^2$ and $5p^6$ electrons. The rare-earth-doped materials are well known for the good luminescent characteristics in visible range [1–4]. Yttrium aluminum oxides, such as $Y_3Al_5O_{12}$ (YAG) and $YAlO_3$, are well known as chemically stable optical materials which are suitable hosts for many rare-earth ions [5,6]. The rare-earth ions can easily replace the yttrium ion. Because the properties of yttrium and other rare-earth ions are similar, the concentration of the doping rare-earth ions in yttrium ion oxides can be larger than in other hosts, leading to more efficient and special optical properties.

Yttrium gallium oxides can also be used as the host for rare-earth doping materials because they have similar structure with yttrium aluminum oxides [7,8]. There are four compounds, $Y_3Ga_5O_{12}$, $YGaO_3$, $Y_4Ga_2O_9$ and Y_3GaO_6 in the Y_2O_3–Ga_2O_3 pseudo-binary systems [9–11]. $Y_3Ga_5O_{12}$ is well known as gallium garnet with the space group $Ia\bar{3}d$ [12], while $YGaO_3$ crystallizes in a distorted perovskite structure [10]. The

*Corresponding author. Institute of Physics and Center for Condensed Mater Physics, The Chinese Academy of Sciences, Group A03, P.O. Box 603, Beijing 100080, China. Fax: +86 10 8264 9531.
E-mail addresses: fsliu@aphy.iphy.ac.cn (F.S. Liu), qlliu@aphy.iphy.ac.cn (Q.L. Liu).

0022-4596/$ - see front matter © 2005 Elsevier Inc. All rights reserved.
doi:10.1016/j.jssc.2005.01.007

study on the luminescence of Eu^{3+}-, Tb^{3+}-doped Y_3GaO_6 was reported by Peimin Guo et al. [13]. The optical spectra of Nd^{3+}, Sm^{3+}, Dy^{3+}, Ho^{3+}, Er^{3+} and Tb^{3+}-doped Y_3GaO_6 are reported in our earlier works [14,15].

In this work, we prepared a series of Tm^{3+}-doped $(Y_{1-x}Tm_x)_3GaO_6$ compounds, and refined their crystal structure using X-ray powder diffraction data by means of Rietveld refinement technique. Their optical properties such as PL, excitation, absorption and time-resolved spectra are discussed in detail. The subsolidus phase relation of Y_2O_3–Ga_2O_3–Tm_2O_3 system sintering at 1500 °C is also figured out.

Table 1
Lattice parameter of $(Y_{1-x}Tm_x)_3GaO_6$

Tm content x (%)	a (Å)	b (Å)	c (Å)	V (Å^3)
0	8.8413(1)	11.0953(1)	5.3966(1)	529.39(1)
0.5	8.8401(1)	11.0948(1)	5.3959(1)	529.23(1)
1	8.8401(1)	11.0945(1)	5.3966(1)	529.28(1)
1.5	8.8400(1)	11.0943(1)	5.3964(1)	529.24(1)
2	8.8394(1)	11.0938(1)	5.3961(1)	529.16(1)
2.5	8.8397(1)	11.0943(1)	5.3962(1)	529.21(1)
3	8.8375(1)	11.0912(1)	5.3950(1)	528.81(1)
10	8.8325(1)	11.0856(1)	5.3924(1)	527.99(1)
20	8.8233(1)	11.0745(1)	5.3881(1)	526.49(1)
30	8.8140(1)	11.0630(1)	5.3832(1)	524.91(1)
40	8.8056(1)	11.0531(1)	5.3795(1)	523.58(1)
60	8.8054(1)	11.0530(1)	5.3793(1)	523.58(1)

2. Experiments

Polycrystalline samples were prepared by solid-state chemical reaction. The starting materials are high-purity (>99.99%) Tm_2O_3, Y_2O_3 and Ga_2O_3. The raw powder was preheated separately at 200 °C for 5 h and weighed according to the stoichiometric compositions for the $(Y_{1-x}Tm_x)GaO_6$ and Y_2O_3–Tm_2O_3–Ga_2O_3 ternary system. The composition of the samples is shown in Tables 1 and 2. Then the fully mixed powder was calcined at 900 °C for 12 h in air. After regrinding, the calcined powder was pressed into pellets and sintered in a silicon–molybdenum furnace at 1500 °C for 48 h in air. Finally, the samples were cooled to room temperature with the furnace in the air and then analyzed by X-ray powder diffraction. The samples are ground and sintered repeatedly in order to reach equilibrium according to the invariance of phase components and the lattice parameters of the phase examined by XRD.

Table 2
Phase relation and lattice parameter in Y_2O_3–Ga_2O_3–Tm_2O_3 system

Composition (at%)			Phase relation	Lattice parameter
Ga_2O_3	Tm_2O_3	Y_2O_3		
0	0	100	$(Y_xTm_{1-x})_2O_3$ ($Ia\bar{3}$) complete solid solution	10.6123(1)
0	25	75		10.5821(1)
0	50	50		10.5501(1)
0	75	25		10.5205(1)
0	100	0		10.4931(1)
62.5	0	37.5	$Y_{3+x}Ga_{5-x}O_{12}$	12.2720(1)
61	0	39	$Y_{3+x}Ga_{5-x}O_{12}$	12.2980(1)
60	0	40	$Y_{3+x}Ga_{5-x}O_{12}$	12.3161(1)
59	0	41	$Y_{3+x}Ga_{5-x}O_{12}$	12.3323(1)
50	0	50	$Y_{3+x}Ga_{5-x}O_{12}$ + Y_3GaO_6	12.4383(1)[a]
33.3		66.7	$Y_{3+x}Ga_{5-x}O_{12}$ + Y_3GaO_6	12.4384(1)[a]
62.5	37.5	0	$Tm_{3+x}Ga_{5-x}O_{12}$	12.2259(1)
61	39	0	$Tm_{3+x}Ga_{5-x}O_{12}$	12.2473(1)
60	40	0	$Tm_{3+x}Ga_{5-x}O_{12}$	12.2648(1)
59	41	0	$Tm_{3+x}Ga_{5-x}O_{12}$	12.2819(1)
50	50	0	$Tm_{3+x}Ga_{5-x}O_{12}$ + Tm_2O_3	12.3497(1)[a]
62.5	37.5	0	$(Y_xTm_{1-x})_3Ga_5O_{12}$ ($Ia\bar{3}d$) complete solid solution	12.2231(1)
62.5	30	7.5		12.2316(1)
62.5	18.75	18.75		12.2501(1)
62.5	7.5	30		12.2638(1)
62.5	0	37.5		12.2734(1)
44.55	10.54	44.91	$Y_{3+x}Ga_{5-x}O_{12}$ + Y_3GaO_6	12.4245(1)[a]
44.47	14.66	40.87	$Y_{3+x}Ga_{5-x}O_{12}$ + Y_3GaO_6	12.4233(1)[a]
57.86	10.24	31.9	$(Y_xTm_{1-x})_3Ga_5O_{12}$ SS	12.3419(1)

[a]Lattice parameter of garnet-type solid solution.

XRD data used for structure analysis were collected on a Rigaku D/max 2500 diffractometer with Cu$K\alpha$ radiation (50 kV × 250 mA) and a graphite monochromator. A step scan mode was employed with a step width of $2\theta = 0.02^\circ$ and a sampling time of 1 s in $2\theta = 10-120^\circ$. The lattice parameters of the compounds were refined by the Rietveld refinement program FullProf.2k (Version 2.40) [16] based on the structure model of Y_3GaO_6 reported in our previous work [15] and the well-known garnet and Y_2O_3 structures [18,19]. Pseudo-Voigt function is used as the profile function.

Emission and excitation spectra of $(Y_{1-x}Tm_x)_3GaO_6$ ($x = 0$–0.6) were obtained with an Edinburgh spectrophotometer FLS920 at room temperature (300 K) with a Xe900 Xenon arc lamp, and an nF900 nanosecond flashlamp with a pulse width 1 ns is used to record luminescence decay profile to determine decay time. Absorption spectra were recorded from visible to ultraviolet light wavelength with a Hitachi U-3010 spectrophotometer in a reflection manner using $BaSO_4$ powder as the standard.

3. Results and discussions

3.1. X-ray powder diffractions and structure

3.1.1. $(Y_{1-x}Tm_x)_3$ GaO_6 solid solution

The powder XRD patterns of $(Y_{1-x}Tm_x)_3$ GaO_6 ($x = 0$–0.6) in the region of $2\theta = 30^\circ-45^\circ$ are shown in Fig. 1. The XRD results indicate that the samples for $x = 0-0.3$ are single phase without any impurity; there is a small amount of (about 2%) impurity of $(Y_{1-x}Tm_x)_2O_3$ compound in the sample $x = 0.4$; and there are three phases coexisting in the sample for $x = 0.5$: $(Y_{1-y}Tm_y)_3Ga_3O_{12}$, $(Y_{1-z}Tm_z)_2O_3$ and $(Y_{1-x}Tm_x)_3GaO_6$. It reveals that the solid reaction has reached equilibrium after sintering. The X-ray data of $(Y_{1-x}Tm_x)_3$ GaO_6 could be completely indexed on the basis of an orthorhombic system with space group $Cmc2_1$. Table 1 shows the result of lattice parameters of $(Y_{1-x}Tm_x)_3$ GaO_6 for various Tm content x derived from the Rietveld refinements of the XRD data in the 2θ region of 10–120°. The lattice parameters of Y_3GaO_6 determined in he present work agree well with the previous report [13].

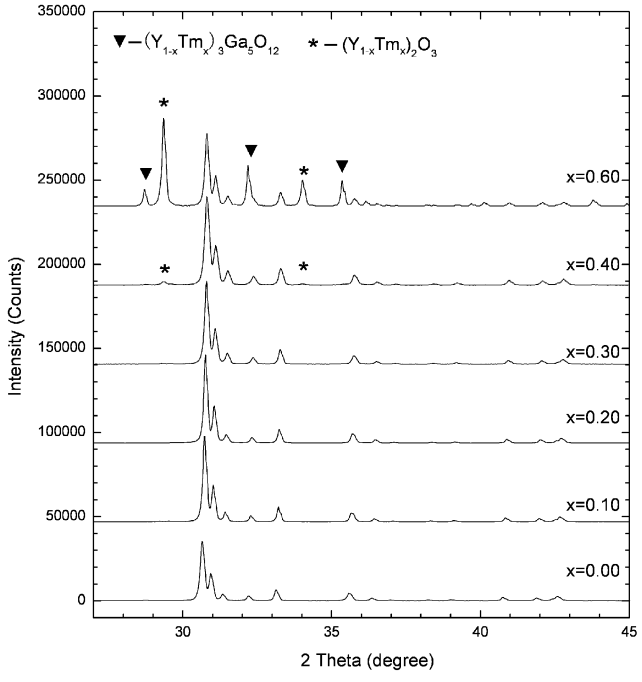

Fig. 1. XRD patterns of $(Y_{1-x}Tm_x)_3GaO_6$.

The lattice parameters of $(Y_{1-x}Tm_x)_3$ GaO_6 for $x = 0.4$ and 0.6 are almost the same, which indicate that the content of Tm_2O_3 in the solid solution $(Y_{1-x}Tm_x)_3$ GaO_6 has reached saturation around $x = 0.4$. Fig. 2 shows variation of the lattice parameters a, b, c and cell volume with the content of thulium in $(Y_{1-x}Tm_x)_3GaO_6$. The lattice parameters decrease linearly with Tm content x, because the ionic radius of Tm^{3+} (0.994 Å, CN = 8) is slightly smaller than that of Y^{3+} (1.019 Å, CN = 8): $a = a_0 - 9.0(1) \times 10^{-2}x$, $b = b_0 - 10.8(1) \times 10^{-2}x$, $c = c_0 - 4.5(1) \times 10^{-2}x$; where a_0, b_0, c_0 are lattice parameters for $x = 0$. This indicates that Tm^{3+} ions substitute for Y^{3+} ions in the lattice. The solid solubility of thulium in $(Y_{1-x}Tm_x)_3GaO_6$ is $x = 0.384$ based on the data in Fig. 2(d).

The structure of $(Y_{1-x}Tm_x)_3$ GaO_6 solid solution is isostructural with Ln_3GaO_6 compounds. There are two sites of 7-fold coordination for Y or Tm atoms with oxygens (Wyckoff position 8b and 4a). Ga atoms are in oxygen tetrahedra (Wyckoff position 4a) which are distorted and elongated along the c-axis [17].

3.1.2. Subsolidus phase relation in Y_2O_3–Ga_2O_3–Tm_2O_3 system

The chemical composition and lattice parameter of samples for Y_2O_3–Ga_2O_3–Tm_2O_3 system are listed in Table 2.

In the Y_2O_3–Tm_2O_3 system, there is one complete solid solution phase $(Y_xTm_{1-x})_2O_3$ with the space group $Ia\bar{3}$. The lattice parameter of the $(Y_xTm_{1-x})_2O_3$ solid solution increases linearly with the increase of the content of Y_2O_3 (Fig. 3b): $a = a_0 + 0.12(1)x$, where a_0 is the lattice parameter of Tm_2O_3.

In the Y_2O_3–Ga_2O_3 system, there is one compound Y_3GaO_6 ($Cmc2_1$) and one solid solution $Y_{3+x}Ga_{5-x}O_{12}$ (YGaGss) with garnet-type structure and space group $Ia\bar{3}d$. The reported $YGaO_3$ does not exist in our system which is synthesized under high pressure [20]. Except the well-known ideal 3:5 molar ratio garnet-type structure $Y_3Ga_5O_{12}$ in the Y_2O_3–Ga_2O_3 system, there also exists a solid solution in a range of Y content. This type of solid

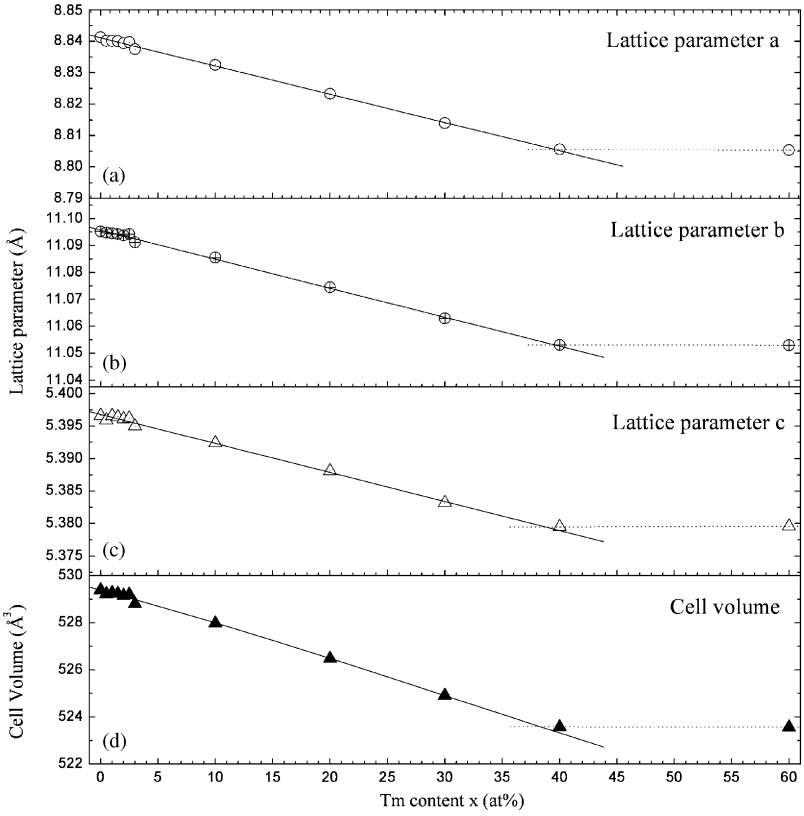

Fig. 2. Variation of the lattice parameters and cell volumes of $(Y_{1-x}Tm_x)_3GaO_6$ with the content of thulium.

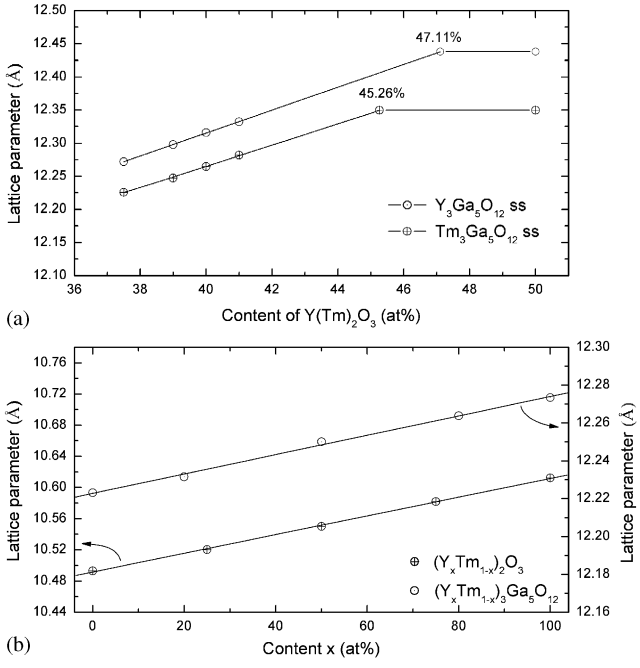

Fig. 3. Variation of lattice parameter of $Y_{3+x}Ga_{5-x}O_{12}$, $Tm_{3+x}Ga_{5-x}O_{12}$, $(Y_xTm_{1-x})_3Ga_5O_{12}$ and $(Y_xTm_{1-x})_2O_3$.

solution of the garnet-type compounds occurs in many Ln_2O_3–Ga_2O_3 and Ln_2O_3–Al_2O_3 systems [21]. The chemical formula of a garnet-type compound can be written as $[A_3]^{3+}[B_2]^{3+}[C_3]^{+3}O_{12}$, where $[A]^{3+}$, $[B]^{3+}$ and $[C]^{3+}$ indicate cations in 8-fold, 6-fold and 4-fold coordination, respectively [22]. In a binary system, the rare-earth cations occupy the A site, and the smaller cations Ga^{3+} or Al^{3+} fill the B and C positions. In the structure of YGaGss, the excess Y^{3+} cations apparently substitute for Ga^{+3} in the octahedral B position. The variation of the lattice parameter of YGaGss with the content of Y_2O_3 is shown in Fig. 3a. The compositional range of Y_2O_3 in YGaGss is 37.5–47.11 at%, which is slightly smaller than that reported by Schneider et al. [9]. The lattice parameter of $Y_3Ga_5O_{12}$ agrees well with the reported data [9,18].

In the Tm_2O_3–Ga_2O_3 system, there is only one solid solution of $Tm_{3+x}Ga_{5-x}O_{12}$ (TGGss) ($Ia\bar{3}d$) with the garnet-type structure. The reported $TmGaO_3$ which is synthesized under high pressure [18] does not exist in our system. The variation of the lattice parameter of TGaGss with the content of Y_2O_3 is shown in Fig. 3a. The compositional range of Tm_2O_3 in TmGaGss is 37.5–45.26 at%. The lattice parameter of $Tm_3Ga_5O_{12}$ agrees well with the reported data (JCPDS 23-589).

For the $Y_3Ga_5O_{12}$–$Tm_3Ga_5O_{12}$ pseudo-binary system, there is a complete solid solution of $(Y_xTm_{1-x})_3Ga_5O_{12}$. The lattice parameter of the $(Y_xTm_{1-x})_3Ga_5O_{12}$ solid solution changes linearly with the increase of the content x of Y_2O_3 (Fig. 3b): $a = a_0 + 0.051(1)x$, where a_0 is the lattice parameter of $Tm_3Ga_5O_{12}$.

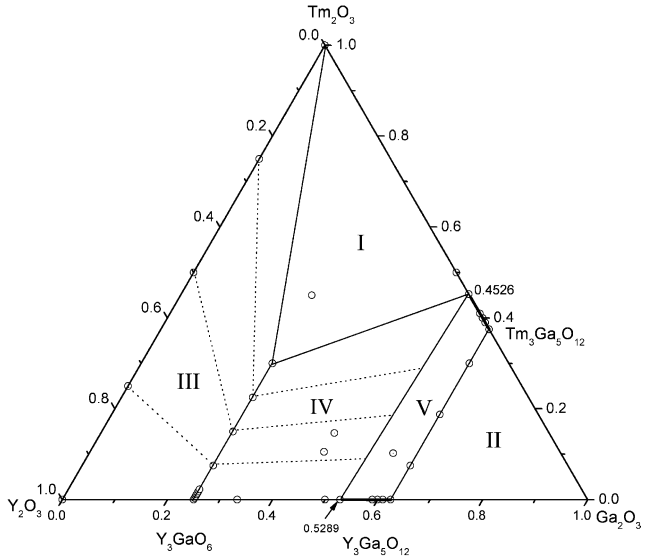

Fig. 4. Subsolidus phase relation in Y_2O_3–Ga_2O_3–Tm_2O_3 system ((I) $Tm_2O_3 + (Y_{0.616}Tm_{0.384})_3GaO_6 + Tm_{3.62}Ga_{4.38}O_{12}$; (II) $(Y_xTm_{1-x})_3Ga_5O_{12}$ SS + Ga_2O_3; (III) $(Y_xTm_{1-x})_2O_3$ SS + $(Y_xTm_{1-x})_3GaO_6$ SS; (IV) $(Y_xTm_{1-x})_3GaO_6$ SS + (Y, Tm)$_3$(Y, Tm, Ga)$_2Ga_3O_{12}$ SS; and (V) (Y, Tm)$_3$(Y, Tm, Ga,)$_2Ga_3O_{12}$ SS).

The subsolidus phase relation of Y_2O_3–Ga_2O_3–Tm_2O_3 pseudo-ternary system under our synthesizing condition is shown in Fig. 4. It can be divided into one three-phase region (I), three two-phase regions (II–IV) and a single phase regions (V). The phase compositions are listed below:

(I) $Tm_2O_3 + (Y_{0.616}Tm_{0.384})_3GaO_6 + Tm_{3.62}\ Ga_{4.38}O_{12}$;
(II) $(Y_xTm_{1-x})_3Ga_5O_{12}$ SS + Ga_2O_3;
(III) $(Y_xTm_{1-x})_2O_3$ SS + $(Y_xTm_{1-x})_3GaO_6$ SS;
(IV) $(Y_xTm_{1-x})_3GaO_6$ SS + (Y,Tm)$_3$(Y,Tm,Ga,)$_2$ Ga_3O_{12} SS (YTGaGss);
(V) (Y,Tm)$_3$ (Y,Tm,Ga,)$_2Ga_3O_{12}$ SS.

3.2. Optic properties of Tm^{3+}-doped Y_3GaO_6

The absorption spectrum of $(Y_{0.60}Tm_{0.40})_3GaO_6$ at room temperature from visible to ultraviolet wavelength are illustrated in Fig. 5. There are four absorption bands centered at 360, 470, 688 and 793 nm, which correspond to the transitions from the ground-state $^3H_6$ to the $^1D_2$, $^1G_4$, $^3F_2 + {}^3F_3$ and $^3H_4$ excited energy levels of thulium, respectively [23]. With the increase of the thulium content, the intensities of the four absorption bands increase. The transition $^3H_6$ to $^3H_4$ resulted in a wide absorption band ranging from 730 to 850 nm. There is a linearly increasing background between 450 and 300 nm, which may correspond to the energy band gap of the Y_3GaO_6 [14]. The transitions from the ground-state $^3H_6$ to higher excited energy such as $^1I_6$ and $^3P_{0-2}$ are not distinguished in the ultraviolet region.

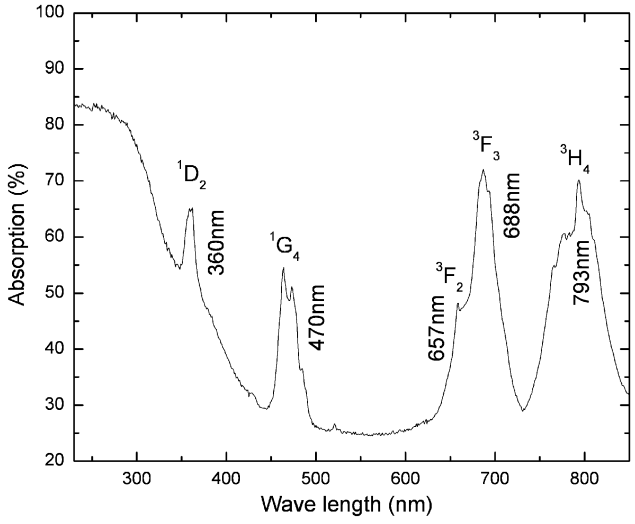

Fig. 5. Absorption spectrum of $(Y_{0.60}Tm_{0.40})_3GaO_6$.

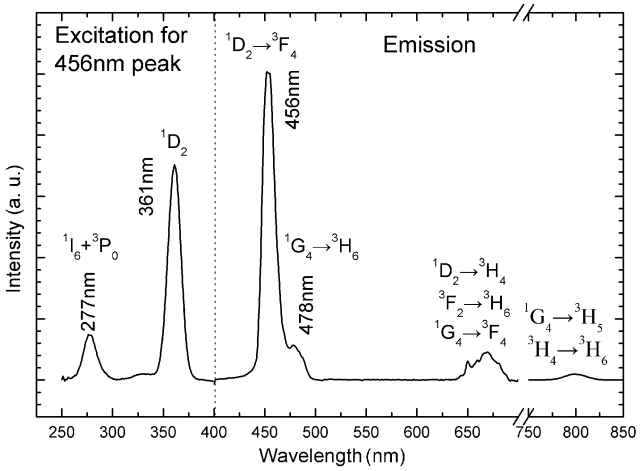

Fig. 6. Excitation for 456 nm peak and emission spectra of $(Y_{0.98}Tm_{0.02})_3GaO_6$, $\lambda e_x = 361$ nm.

The excitation and emission spectra at room temperature of $(Y_{0.98}Tm_{0.02})_3GaO_6$ are shown in Figs. 6 and 7. The strongest emission band in the spectrum is centered at 456 nm with blue color which corresponded to the transitions of $^1D_2 \rightarrow {}^3F_4$ (Fig. 6). Three week emission bands are recorded with the center at 478 and 670 nm when the 361 nm excitation source is used. The band with the center at 478 nm corresponds to the transition of $^1G_4 \rightarrow {}^3H_6$, the 670 nm band corresponds to the transitions of $^1D_2 \rightarrow {}^3H_4$, $^3F_3 \rightarrow {}^3H_6$ and $^1G_4 \rightarrow {}^3F_4$ and the 800 nm band corresponds to the transitions of $^3F_2 \rightarrow {}^3H_6$ and $^3F_3 \rightarrow {}^3H_6$. The blue emission of $^1D_2 \rightarrow {}^3F_4$ at 456 nm is very sharp with the full-width at half-maximum about 12 nm. There are two sharp excitation peaks for the blue emission (456 nm) at 361 and 277 nm, which correspond to the transitions from the ground-state $^3H_6$ to the excited energy level $^1D_2$ and $^1I_6 + {}^3P_0$.

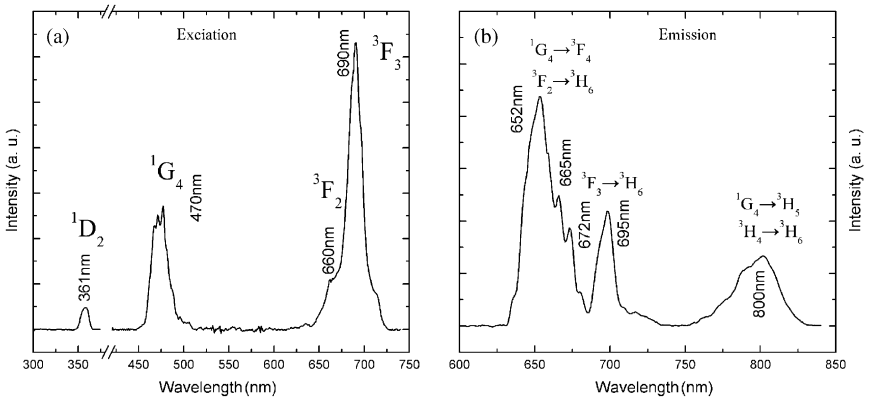

Fig. 7. Excitation for 800 nm peak (a) and emission spectra (b) of $(Y_{0.98}Tm_{0.02})_3GaO_6$, $\lambda e_x = 470$ nm.

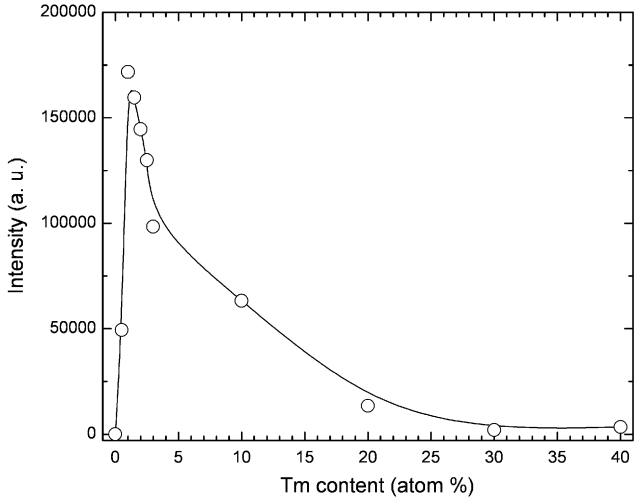

Fig. 8. Relative PL intensity of $^1D_2 \rightarrow {}^3F_4$ transition versus the Tm content x.

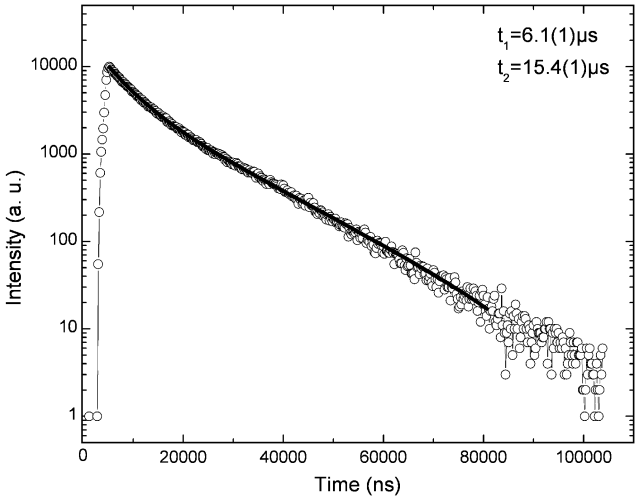

Fig. 9. Luminescence decay of $(Y_{0.98}Tm_{0.02})_3GaO_6$ at room temperature, the fitted profile is shown as black line.

Fig. 7a shows the excitation spectrum for 800 nm emission. There are two strong excitation bands for 800 nm emission with centers at 470 and 690 nm and a relatively week band at 361 nm which corresponds to the transitions from the ground level $^1D_2$ to $^3H_6$, $^3H_6$ to $^1G_4$ and $^3F_2 + {}^3F_3$, respectively. Fig. 7b shows the emission spectrum with the excitation source wavelength of 470 nm. There are three emission bands with the center at 660, 695 and 800 nm, respectively. As shown in Fig. 7b, the 660 nm band corresponds to the transition of $^1G_4 \rightarrow {}^3F_4$, and the other two bands correspond to $^3F_2 \rightarrow {}^3H_6$ and $^3F_3 \rightarrow {}^3H_6$, respectively. Comparing with the blue emission, the intensities of the three emission bands are broad and weak.

The relative intensity of the blue emission at 456 nm versus Tm content x at room temperature is shown in Fig. 8. It shows that there is only a narrow saturation range of PL intensity with the Tm content from $x = 0.005$ to 0.03, and the strongest emission belongs to the Tm content of about 1% atomic ratio. As the Tm content x increases from 0.01 to 0.2, the PL intensity of $^1D_2 \rightarrow {}^3F_4$ transition decreases sharply due to the concentration quenching.

Luminescence decay of $(Y_{0.98}Tm_{0.02})_3GaO_6$ shows two lifetimes for the 456 nm blue emission at room temperature (Fig. 9) for the Tm content $x = 0.02$. The time-resolved spectra can be well characterized as double exponential decays with one very fast component and one slow component. Because of the noise at lower intensity, the data used for the luminescence lifetime fitting are between 5200 and 80000 ns. The fitted profile of the luminescence decay can be expressed by the following equation:

$$y = y_0 + A_1 e^{-x/\tau_1} + A_2 e^{-x/\tau_2}. \quad (1)$$

where $y_0 = -9$, $A_1 = 18200$, $A_2 = 6500$, $\tau_1 = 4.8(1)\,\mu s$, $\tau_2 = 15.4(1)\,\mu s$, The two decay times may be caused by two kinds of coordination positions of the Tm^{3+} ions in the structure. The lifetime of $^1D_2 \rightarrow {}^3F_4$ transition is slightly longer than those of Tm^{3+}-doped $LiTaO_3$ which

are 8 and 4.6 μs for the concentrations at 0.5 and 0.9 at% of Tm^{3+}, respectively [24].

4. Conclusions

In conclusion, the linear change of lattice parameters with the content of Tm reveals that Tm^{3+} replaces the Y^{3+} sites in the $(Y_{1-x}Tm_x)_3GaO_6$ structure. The subsolidus phase relation sintering at 1500 °C is figure out and the solid solubilities of $Y_{3+x}Ga_{5-x}O_{12}$ and $Y_{3+y}Ga_{5-y}O_{12}$ are determined by lattice parameter method. The strong and sharp blue emission at ~456 nm from the $^1D_2 \rightarrow {}^3F_4$ transition shows that Y_3GaO_6 is a potential phosphor and laser crystal host material.

Acknowledgments

This work is supported by the National Natural Science Foundation of China (50372082). The authors thank J.R. Chen for the XRD measurements and Dr. H.W. Dong for the PL measurements.

References

[1] C.X. Guo, W.P. Zhang, C.S. Shi, J. Lumin. 24–25 (Part 1) (1981) 297–300.
[2] M. Breysse, B. Claudel, L. Faure, M. Guenin, J. Lumin. 18-19 (Part 1) (1979) 402.
[3] A. Hoaksey, J. Woods, K.N.R. Taylor, J. Lumin. 17 (1978) 385.
[4] J.I. Pankove, M.A. Lampert, J.J. Hanak, J.E. Berkeyheiser, J. Lumin. 15 (1977) 349.
[5] S. Shinoya, W.M. Yen, Phosphor Handbook, CRC Press, Boca Raton, FL, 1998, p. 515.
[6] K.K. Deb, J. Phys. Chem. Solids 43 (1982) 819.
[7] F.C. Van Rijswijk, R.J.J. Zijlstra, Phys. Lett. A 51 (1975) 271.
[8] E. Rukmini, C.K. Jayasankar, Physica B 212 (1995) 167.
[9] S.J. Schneider, R.S. Roth, J.L. Waring, J. Res. Nat. Bur. Stand. Sect. A 65 (1961) 345.
[10] M. Marezio, J.P. Remeika, P.D. Dernier, Mater. Res. Bull. 1 (1966) 247.
[11] M. Drys, W. Trzebiatowski, Rocz. Chem. 42 (1968) 203.
[12] S. Geller, C.E. Miller, Acta Crystallogr. 13 (1960) 179.
[13] P.M. Guo, G.B. Li, F. Zhao, F.H. Liao, S.J. Tian, X.P. Jing, J. Electrochem. Soc. 150 (2003) H201.
[14] F.S. Liu, Q.L. Liu, J.K. Liang, J. Luo, L.T. Yang, G.B. Song, Y. Zhang, L.X. Wang, J.N. Yao, G.H. Rao, J. Lumin. 111 (1–2) (2005) 61.
[15] F.S. Liu, Q.L. Liu, J.K. Liang, J. Luo, L.T. Yang, G.B. Song, Y. Zhang, L.X. Wang, J.N. Yao, G.H. Rao, Crystal structure and photoluminescence of Tb^{3+} doped Y_3GaO_6, Opt. Mater., in review.
[16] J. R. Carvajal, FULLPROF: a program for rietveld refinement and pattern matching analysis, Abstracts of the Satellite Meeting on Powder Diffraction of the XV Congress of the IUCr, Toulouse, France, 1990, p. 127.
[17] F.S. Liu, Q.L. Liu, J.K. Liang, L.T. Yang, G.B. Song, J. Luo, G.H. Rao, J. Solid State Chem. 177/6 (2004) 1796.
[18] A. Nakatsuka, A. Yoshiasa, S. Takeno, Acta Crystallogr. B 51 (1995) 737–745.
[19] M.G. Paton, E.N. Maslen, Acta Crystallogr. 19 (1965) 307–310.
[20] M. Marezio, J.P. Remeika, P.D. Dernier, Inorg. Chem. 7 (1968) 1337.
[21] M.L. Keith, R. Roy, Am. Miner. 39 (1954) 1–23.
[22] S. Geller, C.E. Miller, Acta Crystallogr. 13 (1960) 179–186.
[23] G.H. Dieke, in: H.M. Crosswhite, H. Crosswhite (Eds.), Spectra and Energy levels of Rare Earth Ions in Crystals, Interscience, New York, 1968, p. 310.
[24] I. Sokolska, W. Ryba-Romanowski, S. Golab, M. Baba, M. Swirkowicz, T. Lukasiewicz, J. Phys. Chem. Solid. 61 (2003) 1573.